The Vertical Distribution of Climate Forcings and Feedbacks from the Surface to Top of Atmosphere

Michael Previdi
Lamont-Doherty Earth Observatory of Columbia University

Beate G. Liepert
NorthWest Research Associates

Submitted to *Climate Dynamics*

April 2011 (revised October 2011)

Corresponding author address:

Dr. Michael Previdi
Lamont-Doherty Earth Observatory of Columbia University
61 Route 9W
Palisades, NY 10964, USA
Phone: (845) 365-8631
E-mail: mprevidi@ldeo.columbia.edu

Abstract

The radiative forcings and feedbacks that determine Earth's climate sensitivity are typically defined at the top-of-atmosphere (TOA) or tropopause, yet climate sensitivity itself refers to a change in temperature at the surface. In this paper, we describe how TOA radiative perturbations translate into surface temperature changes. It is shown using first principles that radiation changes at the TOA can be equated with the change in energy stored by the oceans and land surface. This ocean and land heat uptake in turn involves an adjustment of the surface radiative and non-radiative energy fluxes, with the latter being comprised of the turbulent exchange of latent and sensible heat between the surface and atmosphere. We employ the radiative kernel technique to decompose TOA radiative feedbacks in the IPCC Fourth Assessment Report climate models into components associated with changes in radiative heating of the atmosphere and of the surface. (We consider the equilibrium response of atmosphere-mixed layer ocean models subjected to an instantaneous doubling of atmospheric CO_2.) It is shown that most feedbacks, i.e., the temperature, water vapor and cloud feedbacks, (as well as CO_2 forcing) affect primarily the turbulent energy exchange at the surface rather than the radiative energy exchange. Specifically, the temperature feedback increases the surface turbulent (radiative) energy loss by 2.87 W m^{-2} K^{-1} (0.60 W m^{-2} K^{-1}) in the multimodel mean; the water vapor feedback decreases the surface turbulent energy loss by 1.07 W m^{-2} K^{-1} and increases the surface radiative heating by 0.89 W m^{-2} K^{-1}; and the cloud feedback decreases both the turbulent energy loss and the radiative heating at the surface by 0.43 W m^{-2} K^{-1} and 0.24 W m^{-2} K^{-1}, respectively. Since changes to the surface turbulent energy exchange are dominated in the global mean sense by changes in surface

evaporation, these results serve to highlight the fundamental importance of the global water cycle to Earth's climate sensitivity.

1. Introduction

Climate sensitivity is defined as the equilibrium change in global annual mean surface temperature that occurs in response to a climate forcing, or imposed perturbation of the planetary energy balance. The sensitivity depends critically on the sign and strength of climate feedbacks, which are changes in Earth system properties induced by a climate forcing and acting to either reinforce (for a positive feedback) or counteract (for a negative feedback) the forcing (see, e.g., *Bony et al.*, 2006; *Soden and Held*, 2006; *Previdi et al.*, 2011). Climate forcings and feedbacks have traditionally been evaluated at the top-of-atmosphere (or tropopause), in which case they can also be referred to as radiative forcings and feedbacks, since radiative transfer is the only means by which Earth exchanges energy with space. The reason for considering top-of-atmosphere (TOA) forcings and feedbacks when assessing climate sensitivity is straightforward (see also *Liepert*, 2010). Since the atmosphere effectively has no heat capacity on climate change timescales (i.e., decades or longer), any TOA energy imbalance must be manifest as an equivalent energy imbalance at the surface. In other words, the TOA energy imbalance represents the net heat flux into the surface. Energy added to the surface (for the case of a positive forcing or feedback) goes predominantly into warming the oceans and land, with only a small fraction used to melt ice. Thus, changes in the global mean surface temperature should be proportional to changes in the TOA radiation, and this basic tenet has been the backbone of climate sensitivity research (*Hansen et al.*, 1984). It

is clear from the preceding discussion, however, that TOA forcings and feedbacks must be associated with adjustments in the surface energy balance (e.g., *Liepert et al.*, 2004). Understanding the manner in which these adjustments occur is therefore critical for understanding climate sensitivity. In the current work, we examine the signature of different forcings and feedbacks at the surface, in the atmosphere, and at the TOA, thus providing a consistent picture of changes in energy flow through the atmosphere-surface column.

In contrast to the TOA energy budget, which is purely radiative, the surface energy budget additionally includes a non-radiative component, which consists of the transfer of latent and sensible heat from the surface to the atmosphere. In a global and annual mean sense, this non-radiative (turbulent) energy exchange must balance the net radiative cooling of the atmospheric column, since, as noted above, the atmosphere's heat capacity is negligible. Adjustments in the surface energy balance in response to a climate forcing or feedback can therefore occur in the radiative or non-radiative energy fluxes. *Andrews et al.* (2009) found the non-radiative flux adjustment to be larger than the radiative flux adjustment in a series of climate modeling experiments in which atmospheric CO_2 was instantaneously doubled. (Note that this refers to the direct effect of CO_2 forcing on the surface energy budget; however, we show in subsequent sections that the result also holds for most climate feedbacks.) In particular, *Andrews et al.* (2009) note a reduction in the latent heat flux (LHF) from the surface to the atmosphere that is larger in magnitude than the increase in surface radiative heating. (Changes in the surface sensible heat flux (SHF) were found to be much smaller.) The decrease in surface LHF (which is essentially equal to the decrease in surface evaporation in the

global mean) occurs in order to restore the energy balance of the troposphere, which loses less energy through net longwave (LW) emission when CO_2 levels are higher. This suggests that CO_2 forcing acts to warm the surface primarily by damping the surface evaporative cooling, rather than by enhancing the downward radiation flux from the atmosphere (though the latter effect is certainly not negligible).

The importance of changes in surface evaporation as a mechanism for controlling surface temperature changes has been recognized for some time. For example, *Hartmann and Michelsen* (1993) invoked this mechanism to explain the stability of tropical sea surface temperatures (SSTs) that has been inferred from the geologic record. By stabilizing the tropical SST, evaporation changes also contribute to the polar amplification of surface temperature change predicted by climate models in response to a wide variety of forcings (*Hartmann and Michelsen*, 1993; *Cai and Lu*, 2007). *Joshi et al.* (2008) called upon evaporation effects to explain the land/sea warming contrast that is evident in model simulations of future climate change. Specifically, large areas of the land surface at most latitudes warm more than the surrounding oceans (in both transient and equilibrium simulations), which is due at least partly to the fact that increases in evaporative cooling over land are limited by lack of soil moisture and ecosystem control of evapotranspiration. It is clear from these and other studies that evaporation plays a key role in regulating the surface temperature. In this paper we aim to provide new insight on this issue by assessing quantitatively the impact of different climate feedback processes on the surface energy balance. We show that most feedbacks that are important for climate sensitivity contribute to significant alterations of the turbulent energy loss from

the surface, thus implicating changes in evaporative cooling as a fundamental mechanism controlling the Earth's surface temperature.

2. Methodology

To assess the vertical distribution of different climate feedbacks, we begin by decomposing the global mean TOA radiative perturbation due to each feedback *x* into components associated with changes in radiative heating of the atmosphere (ATM) and of the surface (SFC):

$$dR_x^{TOA} = dR_x^{ATM} + dR_x^{SFC} \quad (1)$$

We consider the equilibrium climate response to an instantaneous doubling of atmospheric CO_2, and evaluate feedbacks resulting from changes in temperature (*T*), water vapor (*q*), clouds (*c*), and surface albedo (*a*), which are the "fast" feedbacks important for climate sensitivity. We further consider the effects of each feedback in isolation, thus neglecting possible interactions between feedbacks. Note that the surface albedo feedback in this case arises entirely from changes in the areal coverage of snow and sea ice. Slower surface albedo feedbacks associated with changes in land ice and vegetation are also important for climate sensitivity (*Previdi et al.*, 2011), but these slow feedbacks are not included here since they are not represented in the climate model experiments we will analyze. Finally, note that dR_x^{TOA} summed over all feedbacks *x* (plus the CO_2 forcing) must equal zero between two equilibrium states; however, this need not be the case for dR_x^{ATM} and dR_x^{SFC} individually.

Recalling from earlier that changes in the global mean atmospheric radiative heating must be balanced by changes in the non-radiative energy transfer from the surface, we can write

$$dR_x^{ATM} = dNR_x^{SFC} \quad (2)$$

where $dNR_x^{SFC} = dLHF_x^{SFC} + dSHF_x^{SFC}$ is the anomalous turbulent energy flux at the surface. Substituting (2) into (1) we obtain

$$dR_x^{TOA} = dNR_x^{SFC} + dR_x^{SFC} \quad (3)$$

which relates a TOA radiative feedback to adjustments in the surface radiative and non-radiative energy fluxes. Equation (3) is thus equivalent to the ocean and land heat uptake induced by feedback *x*.

We compute dR_x^{TOA} and dR_x^{ATM} using the radiative kernel technique (*Soden and Held*, 2006; *Shell et al.*, 2008; *Soden et al.*, 2008; *Previdi*, 2010), and their difference gives us the radiative feedbacks at the surface, dR_x^{SFC}. The radiative kernel technique assumes that feedbacks can be expressed as

$$dR_x^{TOA} = \frac{\partial R^{TOA}}{\partial x} dx \equiv K_x dx \quad (4)$$

and similarly for dR_x^{ATM} and dR_x^{SFC}. K_x in (4) are the radiative kernels, which describe the sensitivity of (in this case) the TOA radiative heating to incremental changes in the feedback variables. Kernels are computed using an offline version of the radiation code from the Max Planck Institute for Meteorology (MPI-M) ECHAM5 general circulation model (GCM), following the approach outlined in *Previdi* (2010). Feedbacks are then calculated by multiplying these kernels by the climate response *dx*, defined here as the change in the feedback variables between the last 10 years of the slab ocean control

experiment and the last 10 years of the $2\times CO_2$ equilibrium experiment in ten different GCMs. These GCMs are listed in Table 1 along with their climate sensitivity for doubled CO_2. Note that equation (4) is used to compute feedbacks resulting from changes in temperature (*T*), water vapor (*q*) and surface albedo (*a*). Nonlinearities associated with clouds preclude the use of the kernel method to estimate cloud feedback, which instead is calculated by adjusting the cloud radiative forcing change (using separate adjustments for the TOA, ATM and SFC) to account for changes to the clear-sky radiative fluxes (*Shell et al.*, 2008; *Soden et al.*, 2008; *Previdi*, 2010). The approach employed in the present study is similar to the one described in *Previdi* (2010). In the latter study, 21st century changes to the atmospheric radiative heating associated with different climate feedbacks were evaluated in transient integrations of the IPCC Fourth Assessment Report (AR4) GCMs. We extend this analysis here using the $2\times CO_2$ equilibrium integrations of the AR4 models, additionally examining the radiative heating changes at the TOA and surface.

Figure 1 shows the zonal and annual mean temperature kernels. Each point in the latitude-height plane represents the effect of a 1 K warming at that point on the radiative heating at the TOA, in the atmosphere, or at the surface. Increases in temperature at all latitudes and heights act to decrease the radiative heating (increase the radiative cooling) for both TOA and ATM, as expected. The impact on the TOA radiative cooling (Fig. 1a) is strongest in a band in the middle to upper troposphere extending from the equator to about 60° latitude in each hemisphere. This region essentially represents the mean level of LW emission to space; temperature increases below it have a smaller effect on the TOA outgoing radiation since the enhanced emission from the lower troposphere is

substantially attenuated as a result of absorption by clouds and water vapor. In contrast, temperature increases in the lower troposphere produce relatively large compensating changes in the ATM and SFC LW radiative energy loss (Figs. 1b,c), enhancing the LW energy loss of the atmospheric column while decreasing net surface LW energy loss by about the same amount. The effect of surface warming on the radiative heating at the TOA, in the atmosphere, and at the surface is illustrated in Figure 2a. Surface LW energy loss increases by approximately 3-4 W m^{-2} per degree of surface warming. However, this is reflected as only a small increase in the TOA LW energy loss (generally < 1 W m^{-2} K^{-1}), since the atmosphere absorbs most of the additional LW flux emitted by the surface, thus decreasing the ATM net LW cooling.

The surface albedo kernels are plotted in Figure 2b. The kernels have been multiplied by -1 in order to show the radiative heating changes resulting from a 1% decrease in albedo. It is evident that albedo changes are felt almost exclusively at the SFC and TOA, with hardly any impact on the ATM radiative heating. This is not surprising given the atmosphere's large transmissivity to shortwave (SW) radiation. The effect of albedo changes is strongest in high latitudes where the surface is bright due to snow and ice cover, although larger increases in SFC and TOA SW heating occur in high southern latitudes than in high northern latitudes. This is partly a result of less cloud cover in high southern latitudes, which enhances the impact of surface albedo changes, but is also due to the fact that a reflective surface (i.e., the Antarctic ice sheet) persists throughout the year (whereas in high northern latitudes snow and sea ice melt during the summer months when SW radiation is present and albedo changes can have an effect).

At low latitudes, the surface is already absorbing most of the insolation, so a 1% decrease in surface albedo has relatively little effect.

Finally, in Figures 3 and 4, we show the LW and SW components of the water vapor kernels. Following *Soden et al.* (2008) and *Previdi* (2010), the *q* kernels have been scaled by the factor

$$\xi \equiv \frac{q}{q_s}\frac{dq_s}{dT} \tag{5}$$

where q_s is the saturation specific humidity calculated from the monthly mean temperature and pressure at each point. Figures 3 and 4 therefore depict the effect that water vapor increases would have on the radiative heating assuming that the atmosphere warms uniformly by 1 K while maintaining constant relative humidity. Increasing atmospheric water vapor concentrations reduces the outgoing LW radiation at the TOA (Fig. 3a), particularly when the water vapor increases occur in the subtropical upper troposphere. Increases in *q* in this region also reduce the LW cooling of the atmospheric column (Fig. 3b). In contrast, higher water vapor amounts in the lower troposphere enhance the downwelling LW flux to the surface, thus increasing the ATM LW cooling while decreasing the SFC cooling (Figs. 3b,c). This effect is strongest in the tropics slightly above the surface (at ~ 900 hPa), since at tropical surface temperatures the water vapor emission is already nearly saturated. Higher water vapor concentrations lead to greater SW absorption in the atmosphere at the expense of the surface (Figs. 4b,c). The ATM and SFC SW heating changes do not completely cancel one another, however, resulting in a small increase in heating at the TOA (Fig. 4a).

3. Results

In this section we examine the signature of different climate feedbacks at the TOA, in the atmosphere, and at the surface. Figure 5 shows the global annual mean *T*, *q*, *c* and *a* feedbacks for the models listed in Table 1. Feedbacks have been normalized by the global mean surface air temperature change, and have been vertically integrated from the surface to the tropopause, defined as 100 hPa at the equator and increasing linearly with latitude to 300 hPa at the poles.

The most fundamental stabilizing (negative) climate feedback is the temperature feedback, whereby increases in temperature (in response to a positive climate forcing) cause the planet to emit more LW radiation to space. In the multimodel mean, this additional LW energy loss amounts to 3.47 W m^{-2} K^{-1}, the majority of which (83%, or 2.87 W m^{-2} K^{-1}) is due to greater emission from the atmosphere (Fig. 5a). Surface LW energy loss increases only slightly (by 0.60 W m^{-2} K^{-1}), since the enhanced upward LW flux from a warmer surface is largely compensated for by enhanced downward flux from a warmer atmosphere. In contrast, the loss of non-radiative energy from the surface increases much more dramatically in response to warming (by 2.87 W m^{-2} K^{-1}, which is the amount needed to balance the increase in atmospheric radiative cooling).

Figure 5b shows the vertical distribution of the water vapor feedback. Higher water vapor concentrations increase the radiative heating at the TOA by 1.96 W m^{-2} K^{-1} on average in the models, with most of this additional heating (55%, or 1.07 W m^{-2} K^{-1}) felt within the atmosphere. Increases in *q* therefore act to warm the surface in two ways: by enhancing the SFC radiative heating by 0.89 W m^{-2} K^{-1} (which represents the net effect of a 1.46 W m^{-2} K^{-1} increase in downward LW and a 0.57 W m^{-2} K^{-1} decrease in downward SW), and by reducing the SFC turbulent energy loss by 1.07 W m^{-2} K^{-1}.

The cloud feedback is depicted in Figure 5c for the seven models that had the necessary data. All models have a positive *c* feedback at the TOA, but the models differ substantially in terms of how this TOA radiative perturbation is distributed between the atmosphere and surface. In the multimodel mean, however, the effect of cloud changes is to increase the radiative heating of the atmosphere by 0.43 W m^{-2} K^{-1} and decrease the radiative heating of the surface by 0.24 W m^{-2} K^{-1}. This implies that cloud changes warm the surface by diminishing the turbulent energy transfer to the atmosphere.

In contrast to the other feedbacks discussed so far, the *a* feedback is felt almost entirely at the surface (Fig. 5d). In other words, albedo changes have essentially no effect on the atmospheric radiative heating, thus indicating a negligible impact on the surface non-radiative energy flux.

The spatial distributions of the different feedbacks are plotted in Figures 6 and 7. The temperature and water vapor feedbacks (Fig. 6) are strongest in the tropics for both TOA and ATM. Increases in temperature produce the largest increase in surface net LW cooling over the continents and at high latitudes, whereas over the oceans the SFC LW cooling increases much less or even decreases (Fig. 6c). This is partly a result of enhanced surface warming over land and in the Arctic, and is also due to the fact that the LW emissivity of the atmosphere in these areas is smaller than over the oceans (mainly because of less water vapor), implying a smaller increase in the surface downwelling LW radiation. The water vapor feedback at the TOA and in the atmosphere (Figs. 6d,e) has a maximum over the eastern equatorial Pacific. This is associated with a lack of high clouds in this region and thus a strong impact of upper tropospheric moistening on the outgoing LW flux at the TOA. Cloud feedbacks, although quite noisy, are generally

positive for TOA and ATM (Figs. 7a,b) with the exception of over the Arctic and high latitude Southern Ocean. At the SFC (Fig. 7c), cloud changes decrease the radiative heating in the subpolar North Atlantic and Pacific, the equatorial Pacific, and the high latitude Southern Ocean, and increase the radiative heating in the Arctic and Antarctic and in the subtropical oceans. Albedo feedbacks are confined to middle and high latitude regions where snow and sea ice disappears (Figs. 7d,f). As noted above, the effect of *a* changes on the ATM radiative heating is negligible (Fig. 7e).

Finally, we wish to make two additional points. First, although we have focused in this section on climate feedbacks, we have also examined the vertical dependence of the CO_2 forcing. Five of the models listed in Table 1 have archived the $2\times CO_2$ radiative forcing at the tropopause, and we have calculated this forcing at the surface using the ECHAM5 radiation code. The multimodel mean tropopause forcing is found to be 3.61 W m^{-2}, and the surface forcing calculated with ECHAM5 is 0.52 W m^{-2}, implying a forcing in the atmosphere (troposphere) of 3.09 W m^{-2}. These results therefore confirm the findings of *Andrews et al.* (2009) that the radiative effects of doubling CO_2 are experienced mainly in the atmospheric column, thus driving a reduction in the non-radiative energy flux from the surface to the atmosphere. This leads into the second point which we wish to address. In principle, a change in the atmospheric radiative cooling induced by a climate forcing or feedback could be balanced by a change in either the surface LHF or SHF, or some combination of the two. We find that the global annual mean atmospheric radiative cooling increases by 4 W m^{-2} between the slab ocean control experiment and the $2\times CO_2$ equilibrium experiment (based on the average of seven models that had the necessary data to compute this quantity). The LHF from the surface

to the atmosphere increases by 5.27 W m^{-2}, while the SHF decreases by 1.23 W m^{-2}. Thus, adjustments in the surface turbulent energy transfer are dominated by changes in surface evaporation, with SHF changes playing a secondary role.

4. Discussion and Conclusions

The traditional approach to understanding Earth's climate sensitivity has concentrated on the processes (forcings and feedbacks) that perturb the top-of-atmosphere radiative energy balance. While there is good physical reason for this, as discussed in the Introduction, the current work and other studies (e.g., *Liepert*, 2010) have argued that the traditional paradigm should be expanded to also consider the energy balance of the coupled surface-troposphere system. We have presented a simple framework which allows TOA radiative forcings and feedbacks to be directly associated with adjustments in the surface radiative *and* non-radiative energy fluxes, therefore providing an alternative perspective on how these forcings and feedbacks actually work to change the surface temperature. We find that CO_2 forcing and most of the (fast) feedbacks it induces (i.e., temperature, water vapor, and cloud) have larger impacts on the surface non-radiative energy transfer than the radiative energy transfer. In a global mean sense, adjustments in the surface non-radiative energy transfer are dominated by changes in the latent heat flux (rather than the sensible heat flux), thus pointing to a key role for evaporative cooling (i.e., phase transition) in regulating the surface temperature. This importance of evaporative cooling stems from the fact that the *radiative* effects of CO_2 forcing and most feedbacks are felt primarily within the atmosphere, therefore requiring

surface evaporation to respond in order to restore the atmospheric energy balance (since the atmosphere is unable to absorb heat on climate change timescales).

Clearly, many of the individual pieces of the story that is told here were already in place. TOA feedbacks based on radiative kernels have been discussed elsewhere, e.g., by *Soden et al.* (2008); however, *Soden et al.* (2008) do not show results for the atmospheric column or surface, so it is unclear how the TOA radiation changes they discuss are distributed between these two components. *Previdi* (2010) examines the impact of different climate feedbacks on the atmospheric radiative heating, but does not show results for the TOA or surface; thus, it is unclear how the inferred changes in surface turbulent energy transfer due to each feedback compare in sign and magnitude to the changes in surface radiative energy transfer. Note that it is not appropriate to use the TOA results from *Soden et al.* (2008) and the atmospheric results from *Previdi* (2010) to infer surface radiation changes; doing so can be misleading. For example, the multimodel mean TOA cloud feedback reported by *Soden et al.* (2008) is 0.70 W m^{-2} K^{-1}, whereas the multimodel mean atmospheric cloud feedback reported by *Previdi* (2010) is 0.15 W m^{-2} K^{-1}. This would suggest that cloud changes act to increase the radiative heating at the surface by 0.55 W m^{-2} K^{-1}, which is exactly opposite to our finding in the present study that cloud changes decrease surface radiative heating (by 0.24 W m^{-2} K^{-1}). Thus, there is value in examining the TOA, atmospheric and surface feedbacks within a consistent framework (e.g., using a single set of kernels and model experiments). Finally, *Andrews et al.* (2009) discuss how the radiative effects of doubling CO_2 are partitioned between the atmosphere and surface, drawing implications for the hydrological cycle; however, they do not include a similar discussion for the various climate feedbacks,

which are more important for climate sensitivity than the direct effects of CO_2 forcing. Therefore, the current work is the first to simultaneously quantify how CO_2 forcing and all important (fast) climate feedbacks impact the radiative heating at the TOA, within the atmosphere, and at the surface, thus allowing for a clean assessment of the relative importance of surface radiative and non-radiative flux adjustments in driving surface temperature changes.

Our findings suggest that surface temperature responds to increases in atmospheric CO_2 as follows. CO_2 forcing produces an initial warming of the surface-troposphere system. At the surface, this warming is driven partly by an increase in the downwelling LW radiation from the atmosphere, but more so by a decrease in the surface evaporative cooling (see also *Andrews et al.*, 2009). As the planet warms, surface evaporation begins to increase again in order to compensate for the enhanced level of atmospheric LW energy loss. Evaporation increases therefore act to stabilize the surface temperature, and this feedback is more powerful than the increase in surface net LW cooling, which is relatively small due to the stronger downward LW flux emitted by a warmer atmosphere. As climate change progresses, additional feedbacks associated with increases in atmospheric water vapor, decreases in snow and sea ice, and changes in clouds come into play. These feedbacks are positive in the current generation of atmosphere-ocean GCMs examined here, indicating that they increase the radiative heating of the Earth system and thus contribute to further surface warming. The snow and sea ice albedo feedback warms the surface by enhancing surface absorption of SW radiation. The water vapor and cloud feedbacks, however, have larger impacts on the surface non-radiative energy transfer. (As noted above, cloud changes actually *decrease*

the surface radiative heating in the multimodel mean, which one might not expect *a priori*.) This suggests that water vapor and cloud changes are positive feedbacks on the surface temperature primarily because they act to damp the rate of increase in surface evaporation with warming.

While the above is admittedly a simplified thermodynamic description of how the climate system works, it is obvious that the feedbacks controlling climate sensitivity must involve changes in the global water cycle. We have focused in this paper on the impacts of different feedbacks on surface evaporation; however, it is clear that the nature of this interaction is not one-way. In other words, the TOA feedbacks discussed here would not occur in the first place were it not for changes in evaporation and other water cycle processes. For example, one characteristic of the temperature feedback is enhanced warming in the tropical upper troposphere, which is a result of stronger condensational heating. The water vapor, cloud and albedo feedbacks similarly involve changes in the cycling and storage of water in different phases and in different parts of the climate system. Radiative feedbacks are therefore at once a driver of and a response to changes in the water cycle. We suggest that water cycle changes need to be viewed as fundamental in determining the sensitivity of Earth's climate to an imposed forcing, in contrast to the traditional paradigm in which the water cycle is thought to merely respond to surface temperature changes.

Acknowledgments. We thank two anonymous reviewers for helpful comments on the manuscript.

References

Andrews, T., P. M. Forster, and J. M. Gregory, 2009: A surface energy perspective on climate change. *J. Clim.*, **22**, 2557-2570.

Bony, S., R. Colman, V. M. Kattsov, R. P. Allan, C. S. Bretherton, J. –L. Dufresne, A. Hall, S. Hallegatte, M. M. Holland, W. Ingram, D. A. Randall, B. J. Soden, G. Tselioudis, and M. J. Webb, 2006: How well do we understand and evaluate climate change feedback processes? *J. Clim.*, **19**, 3445-3482.

Cai, M., and J. Lu, 2007: Dynamical greenhouse-plus feedback and polar warming amplification. Part II: meridional and vertical asymmetries of the global warming. *Clim. Dyn.*, **29**, 375-391.

Hansen, J., A. Lacis, D. Rind, G. Russell, P. Stone, I. Fung, R. Ruedy, and J. Lerner, 1984: Climate sensitivity: Analysis of feedback mechanisms. In *Climate Processes and Climate Sensitivity*, AGU Geophysical Monograph 29, Maurice Ewing Vol. 5. J. E. Hansen and T. Takahashi, Eds. American Geophysical Union, pp. 130-163.

Hartmann, D. L., and M. L. Michelsen, 1993: Large-scale effects on the regulation of tropical sea surface temperature. *J. Clim.*, **6**, 2049-2062.

Joshi, M. M., J. M. Gregory, M. J. Webb, D. M. H. Sexton, and T. C. Johns, 2008: Mechanisms for the land/sea warming contrast exhibited by simulations of climate change. *Clim. Dyn.*, **30**, 455-465.

Liepert, B. G., 2010: The physical concept of climate forcing. *Wiley Interdisciplinary Reviews: Climate Change*, **1**, 786-802.

Liepert, B. G., J. Feichter, U. Lohmann, and E. Roeckner, 2004: Can aerosols spin down the water cycle in a warmer and moister world? *Geophys. Res. Lett.*, **31**, L06207, doi:10.1029/2003GL019060.

Previdi, M., 2010: Radiative feedbacks on global precipitation. *Environ. Res. Lett.*, **5**, 025211, doi:10.1088/1748-9326/5/2/025211.

Previdi, M., B. G. Liepert, D. Peteet, J. Hansen, D. J. Beerling, A. J. Broccoli, S. Frolking, J. N. Galloway, M. Heimann, C. Le Quéré, S. Levitus, and V. Ramaswamy, 2011: Climate sensitivity in the Anthropocene. *Earth Syst. Dynam. Discuss.*, **2**, 531-550.

Shell, K. M., J. T. Kiehl, and C. A. Shields, 2008: Using the radiative kernel technique to calculate climate feedbacks in NCAR's Community Atmospheric Model. *J. Clim.*, **21**, 2269-2282.

Soden, B. J., and I. M. Held, 2006: An assessment of climate feedbacks in coupled ocean-atmosphere models. *J. Clim.*, **19**, 3354-3360.

Soden, B. J., I. M. Held, R. Colman, K. M. Shell, J. T. Kiehl, and C. A. Shields, 2008: Quantifying climate feedbacks using radiative kernels. *J. Clim.*, **21**, 3504-3520.

Model	Climate Sensitivity (K)
(1) CCCMA T47	3.63
(2) CSIRO MK3_0	3.05
(3) GFDL CM2_0	2.94
(4) GISS ER	2.72
(5) INMCM3	2.01
(6) MIROC MEDRES	3.83
(7) MPI ECHAM5	3.27
(8) MRI	3.16
(9) NCAR CCSM3	2.67
(10) UKMO HADGEM1	4.60

Table 1. List of IPCC Fourth Assessment Report climate models analyzed in the present study. In each case, the atmosphere-mixed layer ocean version of the model was used. Climate sensitivity is defined as the change in global annual mean surface air temperature between the last 10 years of the slab ocean control experiment and the last 10 years of the $2\times CO_2$ equilibrium experiment (with a single realization of each experiment used from each model).

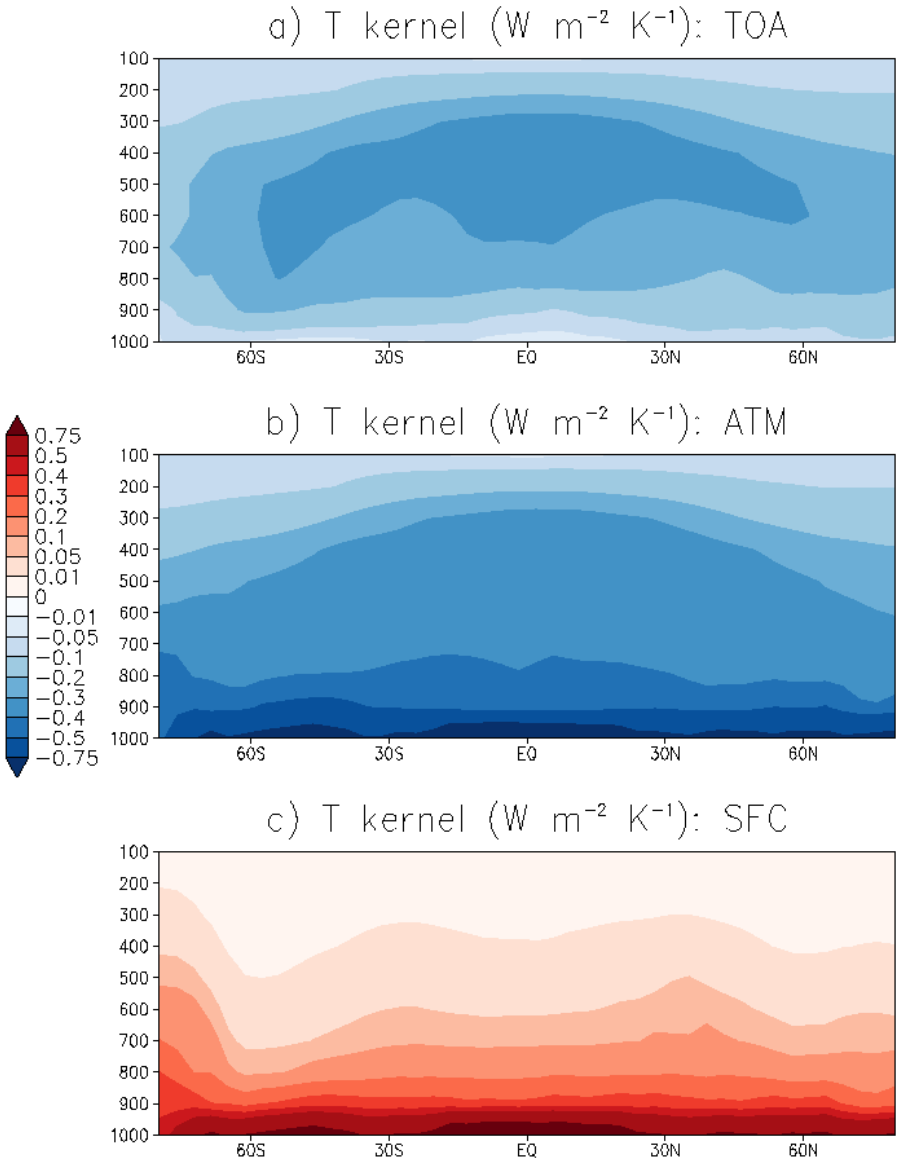

Figure 1. Zonal annual mean temperature kernels for *a)* the top-of-atmosphere (TOA), *b)* atmosphere, and *c)* surface.

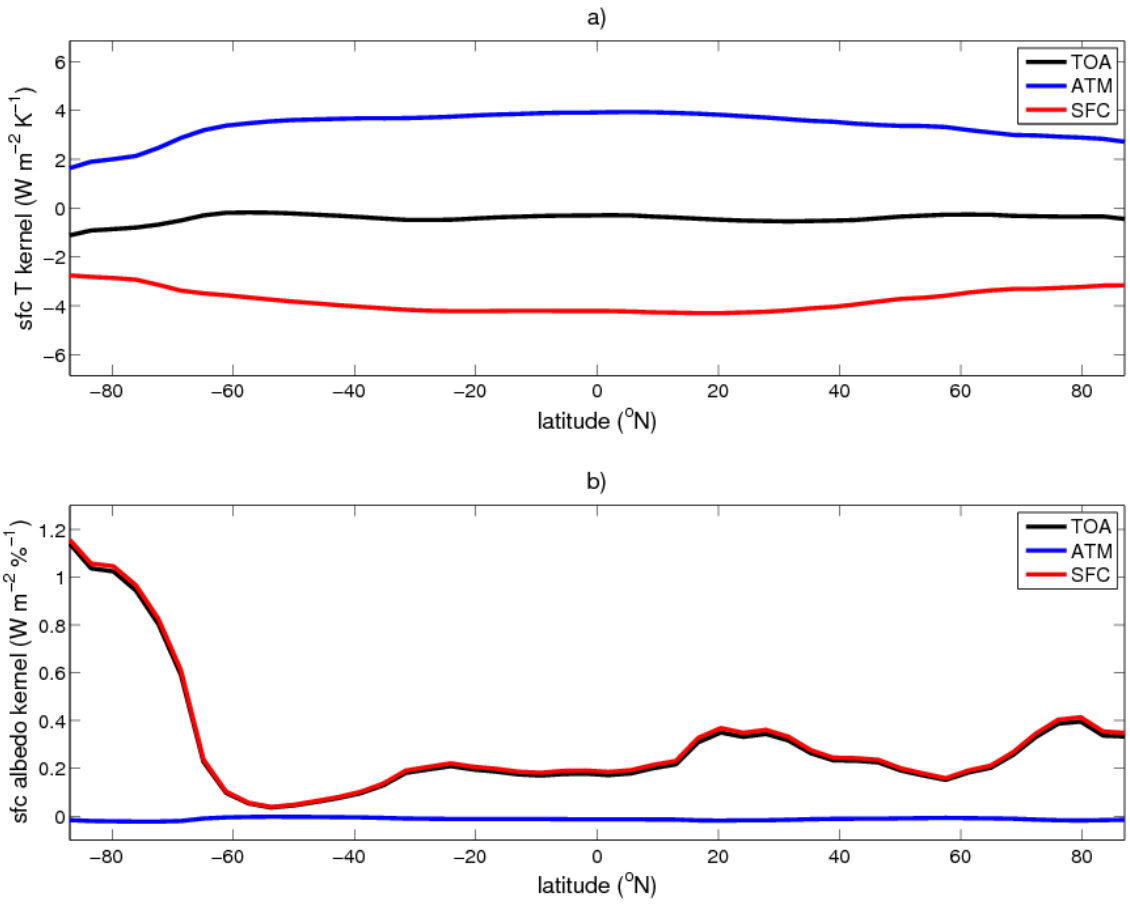

Figure 2. *a)* Surface component of the temperature kernels. *b)* Surface albedo kernels (multiplied by -1).

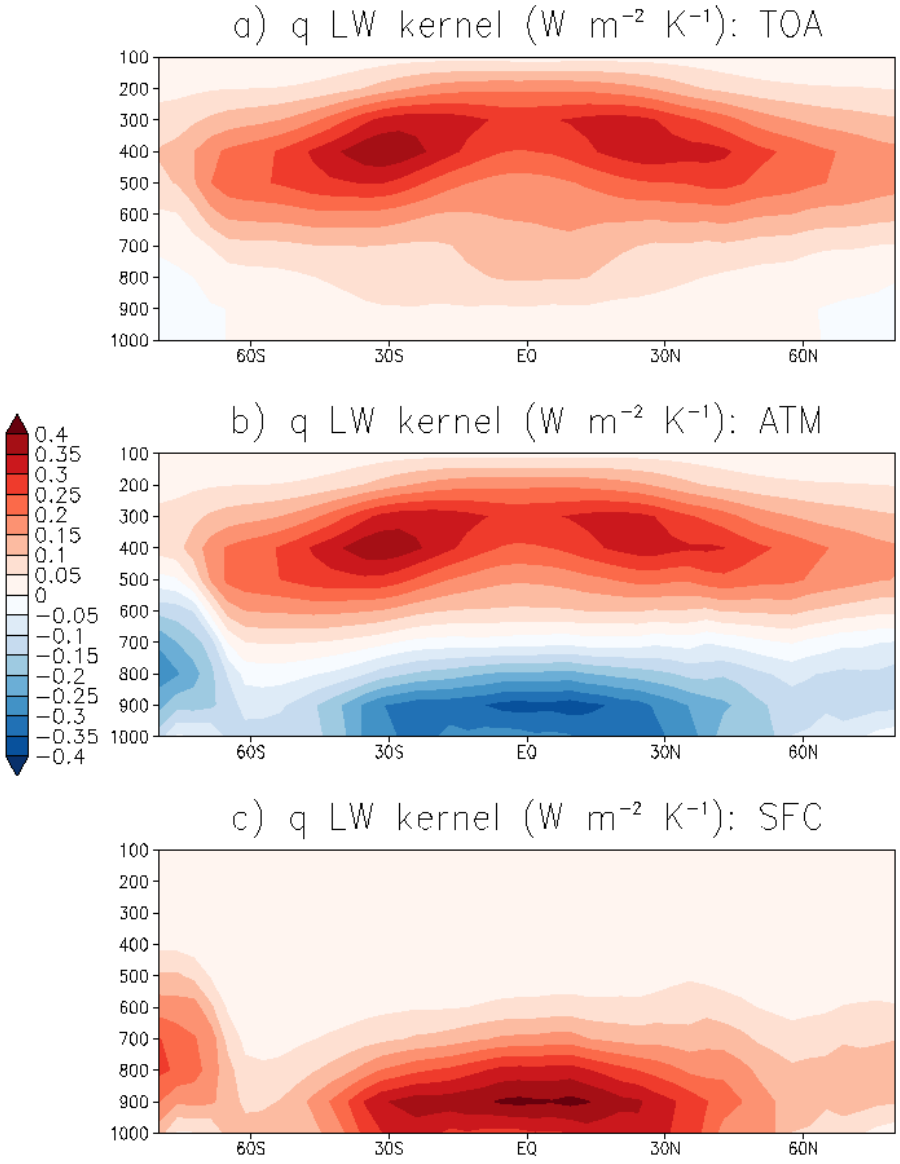

Figure 3. Zonal annual mean longwave water vapor kernels for *a)* the TOA, *b)* atmosphere, and *c)* surface.

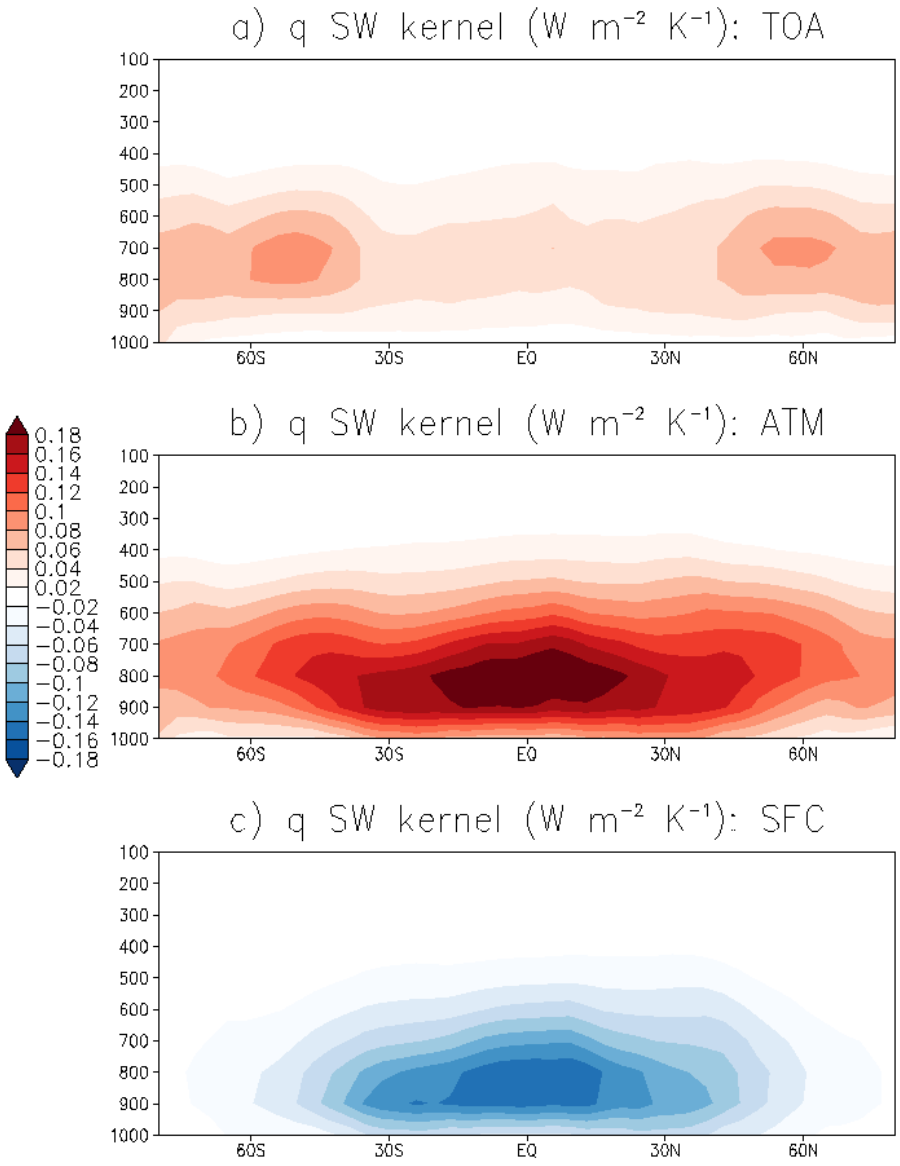

Figure 4. Zonal annual mean shortwave water vapor kernels for *a)* the TOA, *b)* atmosphere, and *c)* surface.

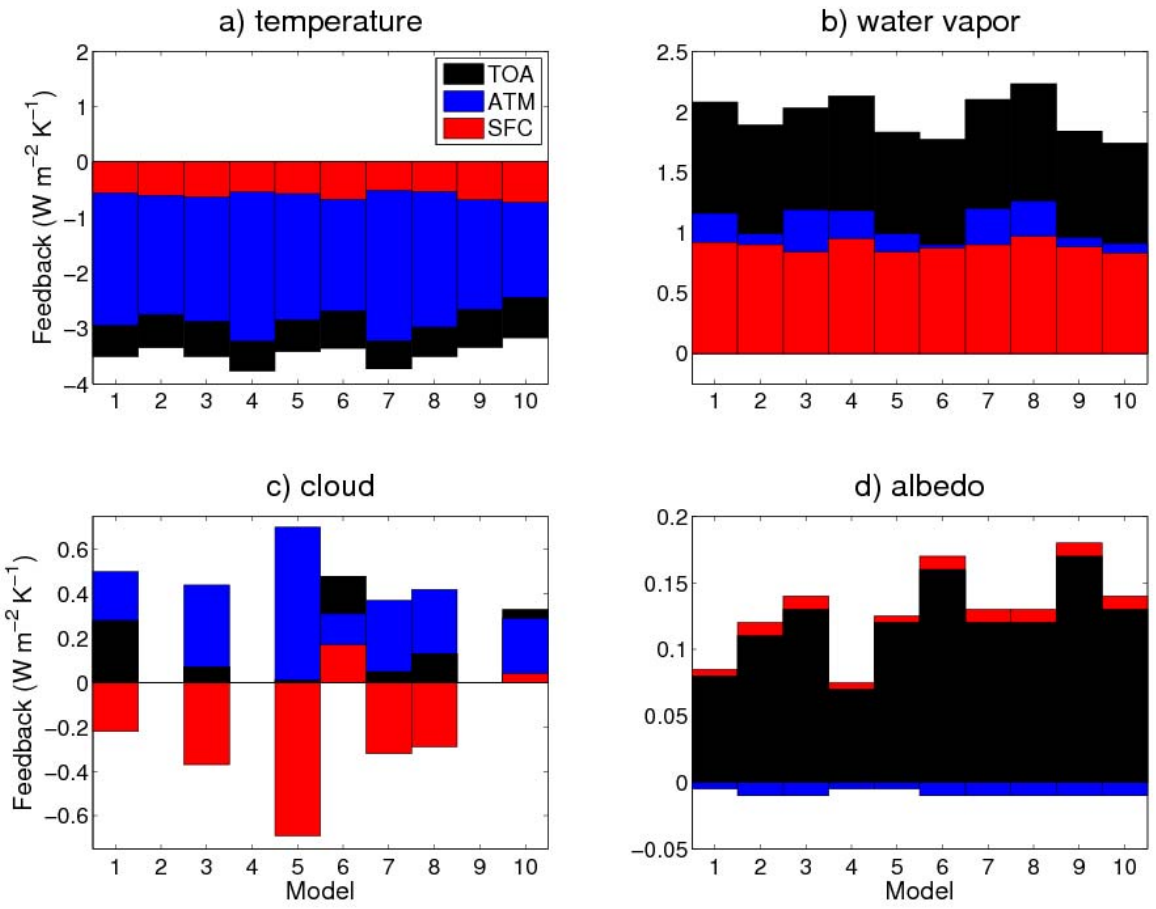

Figure 5. Global annual mean and vertically integrated radiative feedbacks due to changes in *a)* temperature, *b)* water vapor, *c)* clouds, and *d)* surface albedo between the last 10 years of the slab ocean control experiment and the last 10 years of the $2\times CO_2$ equilibrium experiment. Positive values signify an increase in radiative heating at the TOA, in the atmosphere, or at the surface. Numbers along the abscissa correspond to the models listed in Table 1. Note that the bars for TOA, ATM and SFC overlap with one another.

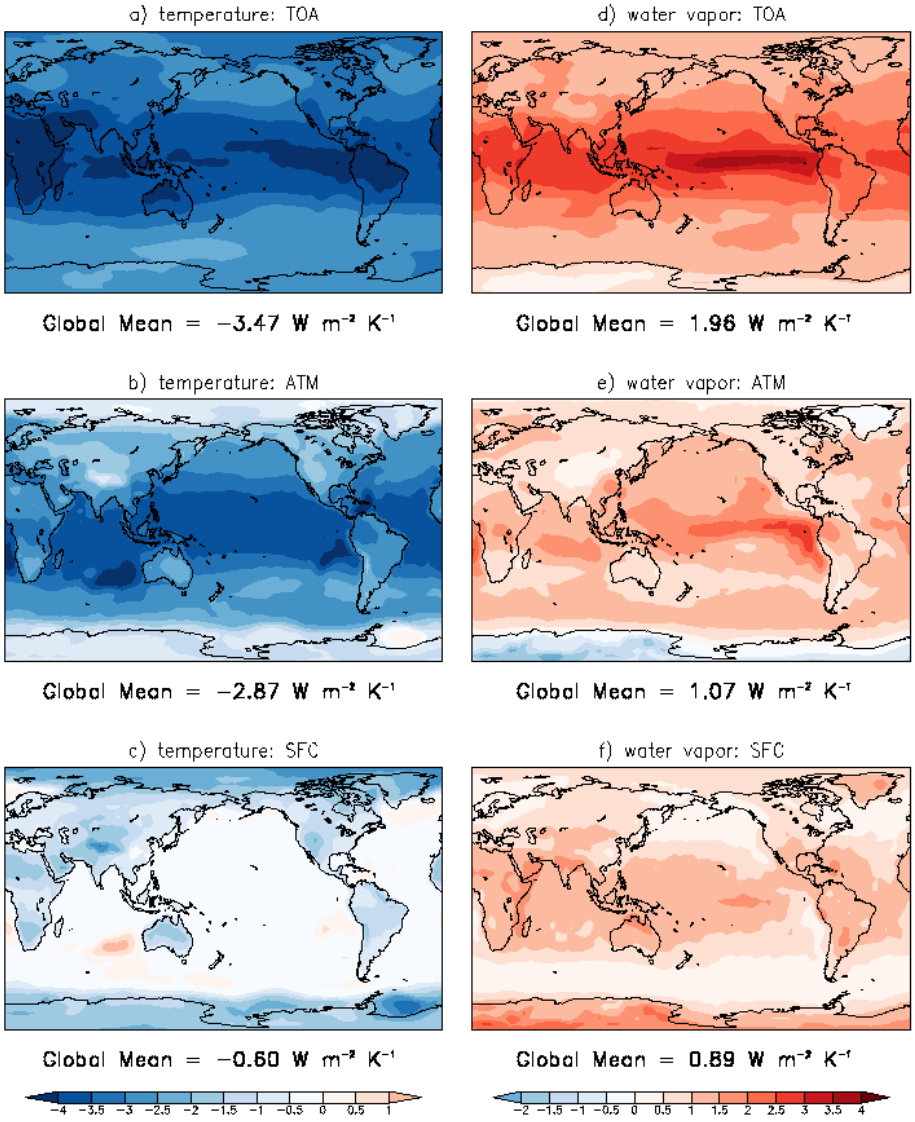

Figure 6. Annual and multimodel mean temperature and water vapor radiative feedbacks at the TOA, in the atmosphere, and at the surface.

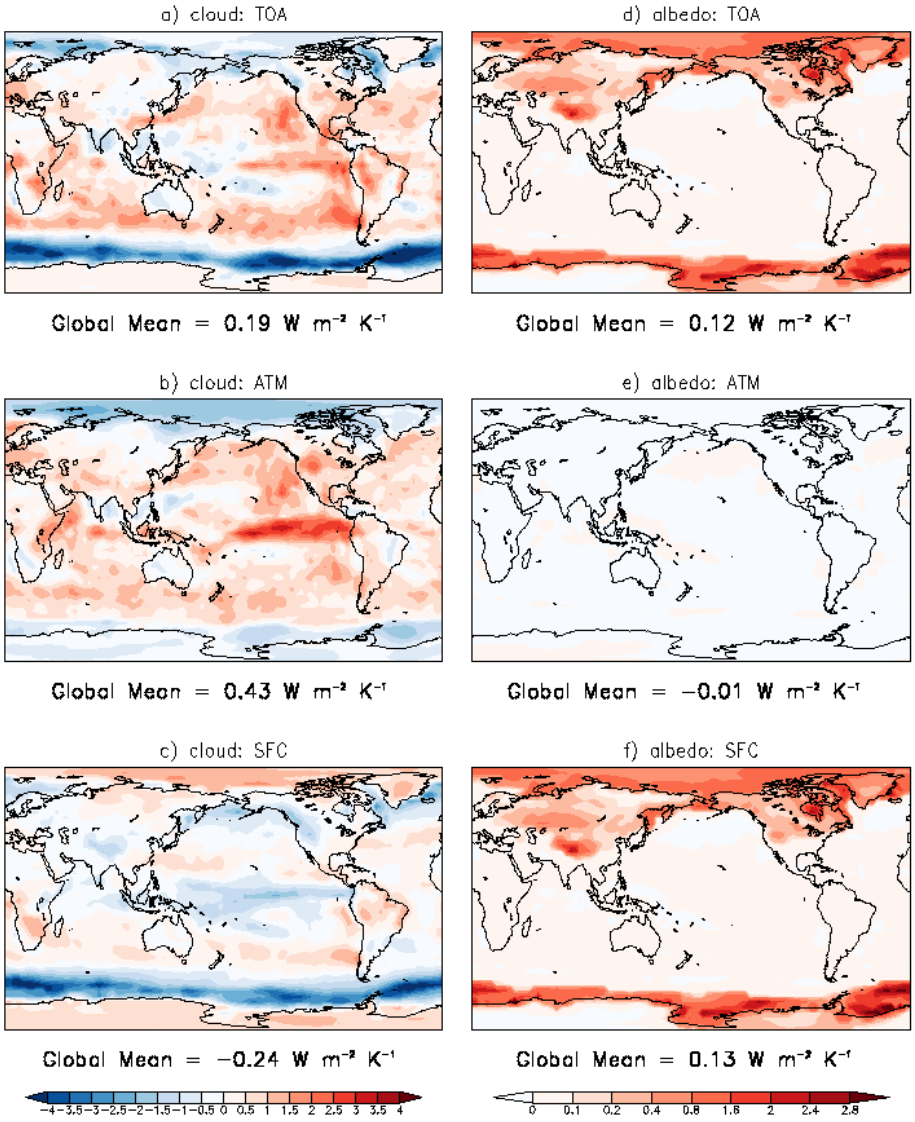

Figure 7. Annual and multimodel mean cloud and albedo radiative feedbacks at the TOA, in the atmosphere, and at the surface.